



Contents lists available at ScienceDirect

Chinese Chemical Letters

journal homepage: [www.elsevier.com/locate/cclet](http://www.elsevier.com/locate/cclet)

Original article

# A nanoporous nitrogen-doped graphene for high performance lithium sulfur batteries

Shuang-Ke Liu\*, Xiao-Bin Hong, Yu-Jie Li, Jing Xu, Chun-Man Zheng\*, Kai Xie

College of Aerospace Science and Engineering, National University of Defense Technology, Changsha 410073, China

## ARTICLE INFO

## Article history:

Received 30 August 2016

Received in revised form 11 October 2016

Accepted 24 October 2016

Available online xxx

## Keywords:

Lithium sulfur battery

Sulfur cathode

Porous graphene

Nitrogen doping

High performance

## ABSTRACT

A nanoporous N-doped reduced graphene oxide (p-N-rGO) was prepared through carbothermal reaction between graphene oxide and ammonium-containing oxometalates as sulfur host for Li–S batteries. The p-N-rGO sheets have abundant nanopores with diameters of 10–40 nm and the nitrogen content is 2.65 at %. When used as sulfur cathode, the obtained p-N-rGO/S composite has a high reversible capacity of 1110 mAh g<sup>-1</sup> at 1C rate and stable cycling performance with 781.8 mAh g<sup>-1</sup> retained after 110 cycles, much better than those of the rGO/S composite. The enhanced electrochemical performance is ascribed to the rational combination of nanopores and N-doping, which provide efficient contact and wetting with the electrolyte, accommodate volume expansion and immobilize polysulfides during cycling.

© 2016 Shuang-Ke Liu, Chun-Man Zheng, Chinese Chemical Society and Institute of Materia Medica, Chinese Academy of Medical Sciences. Published by Elsevier B.V. All rights reserved.

## 1. Introduction

Lithium sulfur (Li–S) battery is regarded as one of the most promising energy storage systems for next generation electric vehicles, due to the high theoretical specific capacity (1672 mAh g<sup>-1</sup>) and high energy density (2600 Wh kg<sup>-1</sup>) of sulfur, which are several times higher than those of the commercial lithium-ion batteries [1–4]. However, the sulfur cathode are facing some big challenges for its practical application. The insulating characteristic of sulfur ( $\sigma = 5 \times 10^{-30} \text{ S cm}^{-1}$  at 25 °C) results in low sulfur utilization and poor rate capability, the dissolution and shuttling effect of the long chain lithium polysulfides (Li<sub>2</sub>S<sub>n</sub>, 4 ≤ n < 8), which are generated during charge and discharge process in liquid electrolytes, lead to the active material loss and deteriorate the cycling performance [1,5].

To address these problems, integrating sulfur with carbon-based materials including micro/mesoporous carbon [6–8], carbon nanofibers [9–11], carbon nanotubes [12–14] and graphene [15–27] have been widely adopted to enhance the electrochemical performance of Li–S batteries. Among these carbon materials, graphene is regarded as an ideal substrate to host sulfur, due to its superior conductivity, high theoretical specific surface area, and excellent mechanical flexibility [17]. In recent years, many efforts

have been made to tailor the pore structure [20–22] or modify the surface chemistry [23–26] of the graphene to host sulfur for enhancing lithium sulfur battery performance. For example, Ding et al. [22] reported a highly porous chemical activated graphene as sulfur host, the existence of nanopores suppressed the polysulfides diffusion and accommodate the volume expansion, resulting in high specific capacity and good cycling stability. Yang et al. [20] and Chen et al. [21] designed a graphene-based layered porous nanostructure and a sandwich-type carbon nanosheets consisting of graphene and micro/mesoporous carbon layer to encapsulate sulfur, respectively. The hierarchical porous carbon layers on graphene sheets could minimize the polysulfide dissolution and shuttling in the electrolyte, thus significantly improve the cycling performance and rate capabilities. Qiu et al. [25] prepared an N-doped graphene using thermal nitridation process in NH<sub>3</sub> atmosphere to wrap S nanoparticles, the as-prepared S@NG demonstrates excellent rate performance and ultralong cycle life up to 2000 cycles, indicating N-doping in graphene could effectively trap lithium polysulfides species and result in stable cycle life.

These results suggest the combination of pore forming and heteroatom doping of graphene is a promising way to develop advanced graphene/S cathode for Li–S batteries. Herein, we present the preparation of a nanoporous N-doped reduced graphene oxide (p-N-rGO) through carbothermal reaction between graphene oxide and ammonium-containing oxometalates as sulfur host for Li–S battery. The nanopores on the graphene sheets were estimated to have diameters of 10–40 nm and the

\* Corresponding authors.

E-mail addresses: [liu\\_sk@139.com](mailto:liu_sk@139.com) (S.-K. Liu), [zhengchunman@hotmail.com](mailto:zhengchunman@hotmail.com) (C.-M. Zheng).<http://dx.doi.org/10.1016/j.cclet.2016.10.038>

1001-8417/© 2016 Shuang-Ke Liu, Chun-Man Zheng, Chinese Chemical Society and Institute of Materia Medica, Chinese Academy of Medical Sciences. Published by Elsevier B.V. All rights reserved.

nitrogen content in the p-N-rGO was 2.65 at%. When used as sulfur cathode, the obtained p-N-rGO/S composite demonstrates a better electrochemical performance compared with those of the rGO/S composite. The rational combination of nanopores and N-doping enables a high reversible capacity of  $1110 \text{ mAh g}^{-1}$  at 1C rate and stable cycling performance with  $781.8 \text{ mAh g}^{-1}$  retained after 110 cycles.

## 2. Results and discussion

Fig. 1 shows the typical preparation process of the p-N-rGO/S composite. The p-N-rGO composite was prepared by a previously reported method [28]. First, the graphene oxide (GO) was prepared from graphite flakes by an improved Hummers method [29], then the GO aqueous solution was mixed well with an ammonium molybdate solution, the dispersed mixture was freeze dried and then annealed at  $900^\circ\text{C}$  under  $\text{Ar}/5\%\text{H}_2$  reduction atmosphere to form the  $\text{MoO}_2@N\text{-rGO}$  composite (Fig. S1a in Supporting information). From Fig. S1a, we could see that large amounts of nanoparticles with diameters much less than 100 nm were anchored on the surface of the wrinkled rGO sheets. The X-ray diffraction patterns prove that the metal oxide nanoparticles are  $\text{MoO}_2$  (Fig. S2 in Supporting information). Second, the  $\text{MoO}_2$  nanoparticles in the composite were etched in the aqueous acid solution to generate p-N-rGO composite (Fig. S1b), on which lots of nanopores are observed. Finally, the p-N-rGO/S composite was synthesized by a solution deposition method.

The microstructure of the p-N-rGO was characterized by transmission electron microscopy (TEM). For comparison, the rGO sample was also prepared by the same method except without adding the ammonium molybdate. Fig. 2 shows the TEM images of the rGO and the p-N-rGO composite. The rGO sample (Fig. 2a) has a smooth morphology without nanopores on its surface, while the p-N-rGO sample (Fig. 2b) shows abundant nano-scaled pores of 10–40 nm on the wrinkled sheets, indicating the nanoporous structure of the p-N-rGO. The pore structures were further analyzed by nitrogen adsorption/desorption isotherm at 77 K. Fig. 3a, b shows the nitrogen adsorption-desorption isotherms and pore size distribution curves of the rGO and p-N-rGO samples. The p-N-rGO shows a high specific surface area of  $321.7 \text{ m}^2 \text{ g}^{-1}$  and a pore volume of  $1.187 \text{ cm}^3 \text{ g}^{-1}$ , while the rGO has a lower specific surface area ( $217.3 \text{ m}^2 \text{ g}^{-1}$ ) and a small pore volume ( $0.963 \text{ cm}^3 \text{ g}^{-1}$ ). From the pore size distribution curves, we could see that there is a remarkable difference ranging from 2 nm to 40 nm in Fig. 3b. This difference is caused by the etching of the  $\text{MoO}_2$  nanoparticles during the preparation of the p-N-rGO, after etched by acid solution, large amounts of nanopores emerge on the graphene sheets, resulting in a dramatic increase of the specific surface area and pore volume (Fig. S3 in Supporting information). The nanoporous structure is beneficial to providing more space for

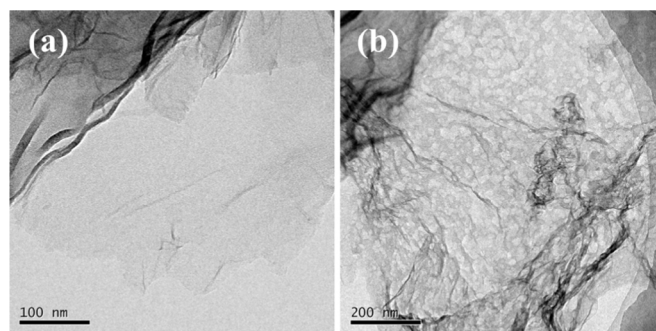


Fig. 2. TEM images of the materials (a, rGO; b, p-N-rGO).

sulfur and volume expansion as well as better accessibility to the electrolyte [22].

To examine surface chemical composition of the rGO and p-N-rGO samples, X-ray photoelectron spectroscopy (XPS) (Fig. 3c) were measured. The rGO sample only shows the C 1s and O 1s signals in the XPS survey spectra at 284.5 eV and 532.5 eV, respectively [30]. As for the p-N-rGO sample, a new peak at 399.5 eV corresponding to N 1s is observed [25,30], indicating the efficient N-doping in the p-N-rGO sample. During the carbothermal reaction, the ammonium molybdate could be thermally decomposed and generate ammonia gas, the ammonia further react with graphene and produce with N functional groups. The atomic ratio of nitrogen in the p-N-rGO sample is estimated to be 2.65% from the peak areas of C 1s, N 1s and O 1s. In the N 1s spectrum (Fig. 3d), the three different peaks at 398.6 eV, 400.9 eV and 405.6 eV are ascribed to pyridinic N, pyrrolic N and chemisorbed N, respectively [31]. The pyridinic N and pyrrolic N types are dominant in the p-N-rGO sample, which are believed to be beneficial to improve the affinity and binding energy of the nonpolar carbon atoms with polar polysulfides/ $\text{Li}_2\text{S}$ , thus alleviating dissolution and shuttle of lithium polysulfides [25,30].

Fig. 4 shows the SEM and TEM images of the p-N-rGO/S composite. From Fig. 4a and b, we could see that after sulfur encapsulation, the p-N-rGO/S composite almost keeps its original morphology without large aggregated sulfur particles observed on the surface of the p-N-rGO sheets. The STEM-EDS mapping (Fig. 4c) further verifies the homogeneous distribution of sulfur and nitrogen throughout the p-N-rGO nanosheets. The sulfur content in the p-N-rGO/S composite is determined through thermogravimetric analysis (TGA) at a heating rate of  $10^\circ\text{C}$  in nitrogen atmosphere. Fig. S4 indicates the p-N-rGO/S composite has a high sulfur content of 69.3 wt%. The XRD pattern in Fig. S5 in Supporting information confirms S in the p-N-rGO/S composite belongs to the orthorhombic sulfur phase (JCPDS card No. 24-0733), which is in agree with previous report [25].

2016 type of coin cells were fabricated to test the electrochemical performance of the p-N-rGO/S and rGO/S electrodes. The cathode electrodes were consisted of 80 wt% S cathodes, 12 wt% carbon Super P and 8 wt% water-soluble binder LA133. The cyclic voltammetry (CV) of the p-N-rGO/S and rGO/S composites were tested at a scan rate of  $0.1 \text{ mV s}^{-1}$ , the results are shown in Fig. 5a. Both electrodes show two well-defined cathodic peaks at  $\sim 2.3 \text{ V}$  and  $\sim 2.0 \text{ V}$  during the first cathodic reduction process, which are attributed to the transformation of cyclo- $\text{S}_8$  to long-chain soluble lithium polysulfides and the further reduction of those polysulfide species ( $\text{Li}_2\text{S}_n$ ,  $4 \leq n < 8$ ) to insoluble short-chain lithium sulfides ( $\text{Li}_2\text{S}_n$ ,  $n \leq 2$ ), respectively. In the following anodic oxidation process, two peaks at 2.35 V and 2.40 V can be observed, corresponding to the oxidation of the lithium sulfides into long-chain polysulfide and eventually to elemental sulfur [31,34]. Though the positions of the cathodic and anodic peaks of the p-N-

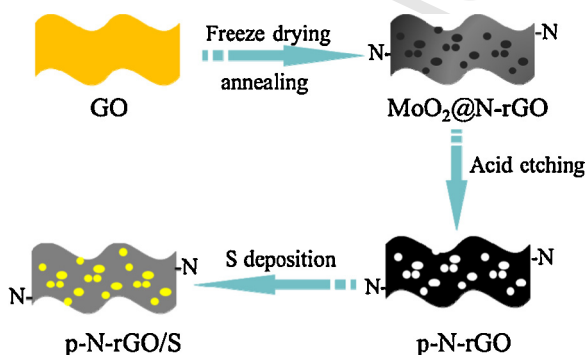


Fig. 1. Schematic illustration for the preparation of p-N-rGO/S composite.

Download English Version:

<https://daneshyari.com/en/article/5143011>

Download Persian Version:

<https://daneshyari.com/article/5143011>

[Daneshyari.com](https://daneshyari.com)